Spin orientation in an exchange coupled Fe/Cr/Fe trilayer determined by polarized neutron reflection

J. A. C. Bland, H. T. Leung, and S. J. Blundell
Cavendish Laboratory, Madingley Road, Cambridge CB3 OHE, United Kingdom

V. S. Speriosu, S. Metin, and B. A. Gurney
IBM Research Division, Almaden Research Center, 650 Harry Road, San Jose, California 95120

J. Penfold
Rutherford-Appleton Laboratory, Chilton 0X11 0QX, United Kingdom

We have used polarized neutron reflection to determine the layer-dependent spin orientations in an antiferromagnetically coupled 100 Å Cr/50 Å Fe/15 Å Cr/50 Å Fe/Si sandwich structure prepared by sputtering. At low field, the net Fe layer magnetic moments align in an asymmetric canted orientation with a near zero total magnetic moment for the sample. At high fields, a canted state, nearly symmetric with respect to the applied field direction is observed and the magnetization in each layer does not reach the bulk saturation value until the layers are ferromagnetically aligned. The behavior is discussed in the context of current theories of exchange coupling. © *1996 American Institute of Physics.* [S0021-8979(96)24908-6]

Exchange coupling in ultrathin transition metal sandwich structures such as Fe/Cr/Fe has been intensively studied, in part because of the giant magnetoresistance (GMR) behavior which can result.[1–4] In addition to the Heisenberg-like bilinear coupling, an additional biquadratic coupling mechanism, favoring a 90° spin alignment has also been found in several epitaxial systems.[5,6] Theoretical models of biquadratic coupling distinguish between an intrinsic mechanism due to the electronic properties of the perfect structure[7–9] and extrinsic mechanisms which predict a strong dependence on the details of the interface morphology and film structure.[10–12] Neutron scattering studies of biquadratic coupling have been previously performed on both polycrystalline FeNi/Ag[13] and Fe/Cr[14] multilayers. Polarized neutron reflection provides an appropriate tool for probing the spin orientation in polycrystalline single trilayers.

We present in this article the results of a detailed polarized neutron reflection (PNR) study of a polycrystalline Fe/Cr/Fe single-sandwich structure with AF coupling.[15] In an earlier study,[16] we were able to show that the spin orientation for such structures occurring at very low field departed significantly from the purely antiparallel structure expected for pure bilinear coupling. In this article the departure from the antiparallel state is quantified. The 100 Å Cr/50 Å Fe/15 Å Cr/50 Å Fe/Si sandwich structures were prepared by sputtering and the field-dependent magnetoresistance behavior investigated as reported previously.[15] X-ray diffraction studies confirm the polycrystalline structure with a preferred (110) texture. Magnetization measurements obtained using a vibrating sample magnetometer (VSM) indicate the presence of antiferromagnetic coupling with saturation and coercive fields of 1.7 and 0.043 kOe, respectively (solid lines, inset of Fig. 1). The saturation value of the moment agrees with that calculated from the bulk magnetization. Measurements made as a function of the in-plane orientation of the applied field confirm the absence of any significant magnetic anisotropy, as expected for such polycrystalline samples.

PNR measurements[17] were made at 300 K with the sample magnetized in-plane and the total specular reflectivity $R^{\pm}$ was determined as a function of perpendicular wave vector q for incident neutron spin parallel $(+)$ and antiparallel $(-)$ to the applied field direction (z axis). The measurements were made at fixed orientation using the CRISP time of flight reflectometer[17] at the ISIS facility in the UK Rutherford Laboratory. As the field is reduced the magnetic moments of the layers move away from the z axis. Both + and − reflectivities are then dependent upon both of the in-plane compo-

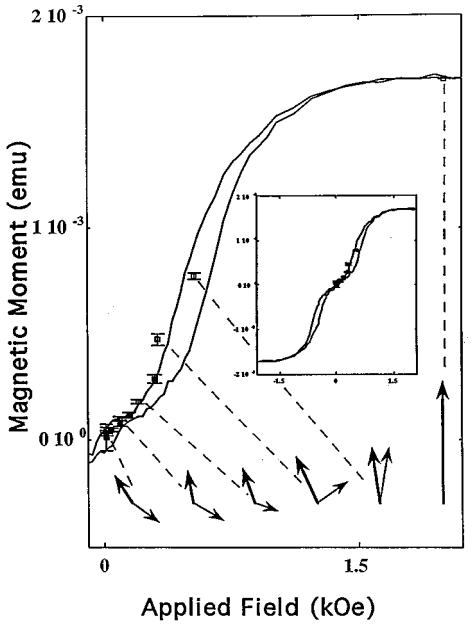

FIG. 1. Magnetization measurements for the positive part of the $M-H$ loop (solid line) for the sputtered 100 Å Cr/50 Å Fe/15 Å Cr/50 Å Fe/Si sample obtained by VSM. The inset shows the full magnetization loop. The net magnetic moment parallel to the applied field deduced from the PNR fits are shown for measurements made upon reducing the applied field from the positive saturation value (open squares) and upon increasing the applied field from the negative saturation value (solid squares). The spin configurations (magnitudes and directions) are drawn to scale as deduced from the coherent multidomain model. The thicker arrow represents the magnetization of the upper Fe layer. The applied field is vertical (z axis).

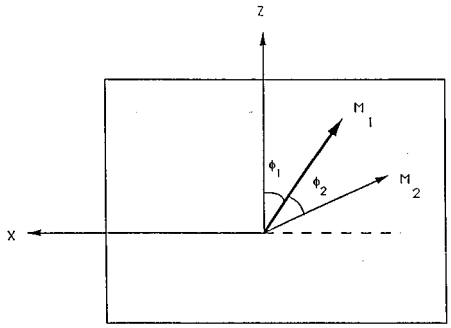

FIG. 2. The sample geometry for a multilayer sample with nonaligned in-plane magnetizations. The first layer magnetization vector $\mathbf{M}_1$ (thick arrow) and the second Fe layer magnetization vector $\mathbf{M}_2$ are constrained to the film plane. The angle ϕ_1 refers to the orientation of $\mathbf{M}_1$ with respect to the applied field direction (vertical z axis) and the angle ϕ_2 defines the angular separation of $\mathbf{M}_1$ and $\mathbf{M}_2$ (narrower arrow), with positive angle corresponding to the anticlockwise sense.

nents of the magnetization vector as described by a reflectivity matrix.[18] A similar description has been given by Felcher *et al.*[19] The magnetic configuration of the sample is shown schematically in Fig. 2. An appropriate spatial averaging procedure is also required since beneath the saturation field magnetic domains can develop.[5] If the domains were larger than the coherence length, then each domain would contribute incoherently to the reflected intensity. The coherence length projected in plane is estimated to be about 100 μm at grazing incidence[17] while Kerr microscopy studies have revealed the existence of an irregular patch domain structure on the scale of a few microns at zero applied field for a trilayer structure with a Cr thickness in the vicinity of the first antiferromagnetic peak (i.e., close to the Cr thickness of our samples) suggesting that coherent averaging applies in our experiment. In a first approximation the net magnetization in each layer then corresponds to the spatial average over the magnetizations of each domain within the coherence area.

The spin asymmetry $S=(R^+-R^-)/(R^-+R^+)$ for $H_a=2$ kOe is consistent with the values calculated for parallel alignment of the two Fe layer moments along the applied field direction.[20] This measurement serves as a check on the experimentally determined layer thicknesses and also on the size of the Fe layer magnetizations which are found to correspond to the bulk value within experimental error. In Fig. 3 we show the spin asymmetry observed evolving as the applied field is reduced from the positive saturation value. The ferromagnetic alignment induces a pronounced peak in the asymmetry at a value of wave vector close to $2.9q_c$ (where q_c is the critical wave vector for the Si substrate). As the applied field is reduced the peak asymmetry at low wave vector diminishes, indicating the expected reduction in the degree of ferromagnetic alignment between the layers, and a second peak close to $6q_c$ increases, as expected from simulations of the spin asymmetry for antiferromagnetic ordering. This peak is related to the antiferromagnetic Bragg diffraction peak that occurs in superlattices,[21,22] although refraction and spin orientation effects must be included in order to accurately fit the position and magnitude of the peak.[18]

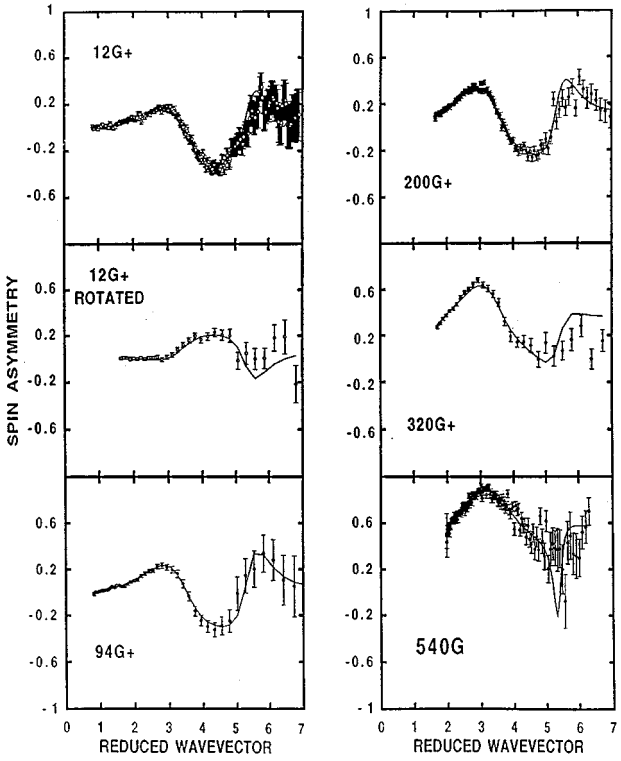

FIG. 3. The spin asymmetry observed for the 100 Å Cr/50 Å Fe/15 Å Cr/50 Å Fe/Si sputtered sandwich structure and the fits (solid lines) predicted by the coherent multidomain model as the applied field is reduced from the positive saturation value to the field strengths indicated. The fit parameters are given in Table I and the resulting spin orientations are shown in Fig. 1.

In fitting the data in the coherent case we relax the requirement that the average magnetization vectors of each layer has the full saturation value $|M_s|$ (corresponding to a single-domain state) and allow both the orientation and size of the magnetization vector in each layer to be determined by the result of a least-squares fit to the asymmetry data. The $S(q)$ curve is computed with the size and orientation of the magnetization vector in each layer treated as independently variable parameters until a close fit (solid line in Fig. 3) is found using a least-squares minimization procedure. This method is found to fit the data very well for the appropriate values of the magnetization vector (magnitude and orientation) in each layer, in contrast to the incoherent averaging method for which no fits could be obtained. The results are summarized in Table I and the resulting spin configurations are shown in Fig. 1. For each configuration shown an alternative symmetry related configuration is also possible corresponding to that obtained by reflecting about the applied field direction. The bold arrow refers to the magnetic moment of the top layer and the thin arrow refers to that of the bottom layer. The resulting component of the magnetization along the applied field ($M_{\|}$ in Table I) fitted using the above procedure is consistent with the magnetometry data on these samples, as shown in Fig. 1. We also find that the angular separation of the magnetic moment vectors is almost exactly preserved under physical rotation of the sample in low-field applied fields (see Table 1 and Fig. 1). This serves as a useful check on our analysis. We see that upon reducing the applied

TABLE I. The result of a least-squares fit to the set of field-dependent spin asymmetry data. The 1st column gives the applied field strength for positive values upon reducing the field from the positive saturation value. The measurement denoted (R) indicates that the sample has been rotated by 90° with respect to the applied field. The angles ϕ_1, ϕ_2 denote the angular position of the top layer magnetization with respect to the applied field and the angular separation of the layer magnetizations. The 4th and 5th columns show the magnitudes of the top and bottom Fe layer moments. The net components of the magnetization parallel and perpendicular to the applied field $M_{\parallel}$ and $M_{\rm per}$ are shown in the final two columns.

H (Oe)	ϕ_1	ϕ_2	M_1/M_s	M_2/M_s	$M_{\parallel}/M_s$	$M_{\rm per}/M_s$
12	−33	160	0.27	0.27	0.032±0.004	0.034±0.039
12R	−110	170	0.26	0.26	0.021±0.002	−0.010±0.011
94	−11	131	0.27	0.29	0.060±0.006	0.100±0.293
200	−19	129	0.30	0.20	0.108±0.005	0.045±0.054
320	−24	79	0.42	0.30	0.278±0.016	0.037±0.062
540	−8	17	0.46	0.46	0.455±0.009	0.004±0.087
2000	0	0	1.00	1.00	1.000	0.000

field from the saturation value, the formation of magnetic domains is inferred (i.e., M_1, M_2 decreases) with, after initial canting away from the applied field direction, the lower Fe layer undergoing a rotation process to attain an overall canted, near AF configuration at low applied fields. Each layer has ~25%–30% of its full saturation magnetization at low fields. We note that from Table I the total magnetic moment of the sample perpendicular to the applied field $|M_{\rm per}|$ is always zero, within experimental error. This is consistent with the physical requirement that for stability there be no net torque on the layers arising from the applied field since the magnetic anisotropy in the sample is negligible. The magnetization reversal process is clearly inequivalent in the two Fe layers, resulting at low field in an asymmetric magnetic orientation with respect to the applied field direction. This inequivalence may result from the inequivalent interfaces of the two Fe layers (the bottom layer is directly deposited on Si).

The canting observed at low field could suggest that in addition to bilinear coupling favoring antiparallel alignment, biquadratic coupling comparable in strength is also present, since in the absence of anisotropy this configuration would be otherwise unstable. In the fluctuation model[10] biquadratic coupling is expected to occur only for sufficiently large terrace widths and appropriate roughness values. For sputtered structures very sharp interfaces can be achieved on the macroscopic scale but the correlation length is expected to be reduced on a nm scale in comparison with epitaxial structures. On the basis of this model, weaker biquadratic coupling would be expected in sputtered samples in contrast with our findings. Other extrinsic models invoking dipolar coupling[12] and the presence of ''loose'' spins[11] in the spacer layer are unlikely to result in the large biquadratic coupling strength we observe. It is also possible that the antiferromagnetism of the Cr layer is important in this context. Alternatively, differences between the Fe layers in net moment, pinning sites or local anisotropy variations together with bilinear coupling could explain the canting without invoking biquadratic coupling. This view is supported by the sample rotation results.

In conclusion, the results demonstrate the importance of determining the layer dependent spin orientation in exchange coupled structures, as is possible using PNR.

[1] G. Binasch, P. Grunberg, F. Saurenbach, and W. Zinn. Phys. Rev. B **39**, 4828 (1989).
[2] J. J. Krebs, P. Lubitz, A. Chaiken, and G. A. Prinz, Phys. Rev. Lett. **63**, 1645 (1989).
[3] A. Fert and P. Bruno, in *Ultrathin Magnetic Structures*, edited by B. Heinrich and J. A. C. Bland (Springer, Berlin, 1994), Chap. 2.2.
[4] S. S. Parkin, in *Ultrathin Magnetic Structures*, edited by B. Heinrich and J. A. C. Bland (Springer, Berlin, 1994), Chap. 2.4.
[5] M. Ruhrig, R. Schafer, A. Hubert, R. Mosler, J. A. Wolf, S. Demokritov, and P. Grunberg, Phys. Status Solidi A **125**, 635 (1991).
[6] B. Heinrich and J. Cochran, Adv. Phys. **42**, 523 (1993).
[7] R. P. Erickson, K. B. Hathaway, and J. R. Cullen, Phys. Rev. B **47**, 2626 (1993).
[8] D. M. Edwards, J. M. Ward, and J. Mathon, J. Magn. Magn. Mater. **126**, 380 (1993).
[9] P. Bruno, J. Magn. Magn. Mater. **121**, 248 (1993).
[10] J. C. Slonczewski, Phys. Rev. Lett. **67**, 3172 (1991).
[11] J. C. Slonczewsi, J. Appl. Phys. **73**, 5957 (1993).
[12] S. Demokrtitov, E. Tsymbal, P. Grunberg, W. Zinn, and I. K. Schuller, Phys. Rev. B **49**, 720 (1994).
[13] R. Rodmacq, K. Dumesnil, Ph. Mangin, and M. Hennion, Phys. Rev. B **48**, 3556 (1993).
[14] M. Schäfer, J. A. Wolf, P. Grünberg, J. F. Ankner, A. Schreyer, H. Zabel, and C. F. Majkrzak, J. Appl. Phys. **75**, 6193 (1994); A. Schreyer *et al.*, Europhys. Lett. (1995) (in press).
[15] B. A. Gurney, D. R. Wilhoit, V. S. Speriosu, and I. L. Sanders, IEEE Trans. Magn. **MAG-26**, 2747 (1990).
[16] J. A. C. Bland, R. D. Bateson, N. F. Johnson, S. J. Blundell, V. S. Speriosu, S. Metin, and B. Gurney, J. Magn. Magn. Mater. **123**, 320 (1993).
[17] J. A. C. Bland, in *Ultrathin Magnetic Structures*, edited by J. A. C. Bland and B. Heinrich (Springer, Berlin, 1994).
[18] S. J. Blundell and J. A. C. Bland, Phys. Rev. B **46**, 3391 (1992).
[19] G. P. Felcher, R. O. Hilleke, R. K. Crawford, J. Haumann, R. Kleb, and G. Ostrowski, Rev. Sci. Instrum. **58**, 609 (1987).
[20] J. A. C. Bland, A. D. Johnson, R. D. Bateson, S. J. Blundell, H. J. Lauter, C. Shackleton, and J. Penfold, J. Magn. Magn. Mater. **93**, 513 (1991).
[21] A. Schreyer, K. Bröhl, J. F. Ankner, C. F. Majkrzak, Th. Zeidler, P. Bödeker, N. Metoki, and H. Zabel, Phys. Rev. B **47**, 15334 (1993).
[22] Y. Y. Huang, G. P. Felcher, and S. S. P. Parkin, J. Magn. Magn. Mater. **99**, L31 (1991).